

Fourth generation effects in rare $B_s \rightarrow \ell^+ \ell^-$ and $B_s \rightarrow \ell^+ \ell^- \gamma$ decays

T. M. Aliev ^{*}, A. Özpineci [†], M. Savcı [‡]

Physics Department, Middle East Technical University
06531 Ankara, Turkey

Abstract

The contribution of the fourth generation quarks to the rare $B_s \rightarrow \ell^+ \ell^-$ and $B_s \rightarrow \ell^+ \ell^- \gamma$ decays are studied. Constraints on the extended Cabibbo–Kobayashi–Maskawa matrix elements $|V_{tb}V_{ts}^*|$ and $|V_{t'b}V_{t's}^*|$ are obtained from the existing experimental result for the branching ratio of the $B \rightarrow X_s \gamma$ decay. The branching ratios of the above-mentioned decays, as well as the photon spectrum in the $B_s \rightarrow \ell^+ \ell^- \gamma$ decay, are studied. It is found that the results are sensitive to the existence of the fourth generation.

PACS number(s): 12.60.–i, 13.20.–v, 13.20.He

^{*}e-mail: taliev@metu.edu.tr

[†]e-mail: altugoz@metu.edu.tr

[‡]e-mail: savci@metu.edu.tr

1 Introduction

The working and forthcoming high-statistics B-physics experiments at BaBar, BELLE, HERA-B, the TeVatron and LHC-B [1] will probe the flavor sector of the Standard Model (SM) with high precision. These experiments may provide hints for the physics beyond the SM. Already, there have been a large amount of theoretical investigations within various scenarios of new physics to calculate the physical observables that will be measured.

The flavor-changing neutral current process $B_{s(d)} \rightarrow \ell^+ \ell^-$ has attracted a lot of attention due to its sensitivity both to the gauge structure of the SM and to the possible new physics beyond SM [2]–[9]. Note that the experimental bound on the branching ratio is [10]

$$\begin{aligned} \mathcal{B}(B_d \rightarrow \mu^+ \mu^-) &< 6.8 \times 10^{-7} \quad (CL = 90\%) , \\ \mathcal{B}(B_s \rightarrow \mu^+ \mu^-) &< 2.0 \times 10^{-6} \quad (CL = 90\%) . \end{aligned}$$

In other words, measuring the branching ratio $B_{s(d)} \rightarrow \ell^+ \ell^-$ can impose the stringiest constraints on the possible parameter space of new physics. The $B_s \rightarrow \ell^+ \ell^- \gamma$ decay is also very sensitive to the existence of the new physics beyond SM. In spite of the fact that this decay has an extra α factor, it was shown in [11, 12] that the radiative leptonic $B_s \rightarrow \ell^+ \ell^- \gamma$ ($\ell = e, \mu$) decays have larger decay rates compared to that purely leptonic ones, while for the τ lepton mode widths for both decays are comparable to each other.

As has already been noted, the flavor-changing neutral current processes $B_s \rightarrow \ell^+ \ell^-$ and $B_s \rightarrow \ell^+ \ell^- \gamma$ are very sensitive to the new physics beyond the SM. One of the most straightforward and economic extension of the SM is adding the fourth generation to the fermionic sector, similar to the three generation case.

Effects of the extra generation to the electroweak radiative correction and its influence on the low energy physics processes were investigated in many works (see for example [13] and references therein).

In this work we study the effects of fourth generation in the $B_s \rightarrow \ell^+ \ell^-$ and $B_s \rightarrow \ell^+ \ell^- \gamma$ decays. The paper is organized as follows. In section 2 we present theoretical description of the $B_s \rightarrow \ell^+ \ell^-$ and $B_s \rightarrow \ell^+ \ell^- \gamma$ decays for the fourth generation case. Section 3 is devoted to the numerical analysis and conclusion.

2 Theoretical background

In this section we will present the necessary theoretical expressions for the $B_s \rightarrow \ell^+ \ell^-$ and $B_s \rightarrow \ell^+ \ell^- \gamma$ decays.

Let us first consider $B_s \rightarrow \ell^+ \ell^-$ decay. At quark level, this decay is described by the $b \rightarrow s \ell^+ \ell^-$ transition for which the effective Hamiltonian can be written as

$$\mathcal{H}_{eff} = \frac{\alpha G_F}{2\sqrt{2}\pi} V_{tb} V_{ts}^* \sum_{i=1}^{10} C_i(\mu) \mathcal{O}_i(\mu) , \quad (1)$$

where the full set of operators in $\mathcal{O}_i(\mu)$ and the corresponding expressions for the Wilson coefficients in the SM are given in [14, 15]. As has been noted earlier, in the model we consider in the present work, the fourth generation is introduced in the same way as the

first three generations are introduced in the SM. The fourth generation changes only values of the Wilson coefficients $C_7(\mu)$, $C_9(\mu)$ and $C_{10}(\mu)$ via the virtual exchange of the fourth generation up quark t' , i.e.,

$$\begin{aligned} C_7^{tot}(\mu) &= C_7^{SM}(\mu) + \frac{V_{t'b}V_{t's}^*}{V_{tb}V_{ts}^*}C_7^{new}(\mu) , \\ C_9^{tot}(\mu) &= C_9^{SM}(\mu) + \frac{V_{t'b}V_{t's}^*}{V_{tb}V_{ts}^*}C_9^{new}(\mu) , \\ C_{10}^{tot}(\mu) &= C_{10}^{SM}(\mu) + \frac{V_{t'b}V_{t's}^*}{V_{tb}V_{ts}^*}C_{10}^{new}(\mu) , \end{aligned} \quad (2)$$

where the last terms in these expressions correspond to the t' quark contributions to the Wilson coefficients and $V_{t'b}$ and $V_{t's}$ are the elements of the 4×4 Cabibbo–Kobayashi–Maskawa (CKM) matrix. The explicit forms of the C_i^{new} can easily be obtained from the corresponding Wilson coefficient expressions in SM by simply substituting $m_t \rightarrow m_{t'}$. The effective Hamiltonian (1) leads to the following matrix element for the $b \rightarrow s\ell^+\ell^-$ transition

$$\begin{aligned} \mathcal{M} &= \frac{G\alpha}{2\sqrt{2}\pi}V_{tb}V_{ts}^*\left[C_9^{tot}\bar{s}\gamma_\mu(1-\gamma_5)b\bar{\ell}\gamma_\mu\ell + C_{10}^{tot}\bar{s}\gamma_\mu(1-\gamma_5)b\bar{\ell}\gamma_\mu\gamma_5\ell \right. \\ &\quad \left. - 2C_7^{tot}\frac{m_b}{q^2}\bar{s}\sigma_{\mu\nu}q^\nu(1+\gamma_5)b\bar{\ell}\gamma_\mu\ell \right] , \end{aligned} \quad (3)$$

where $q^2 = (p_1 + p_2)^2$ and p_1 and p_2 are the final leptons four-momenta. It follows from Eq. (3) that in order to calculate the matrix element for the $B_s \rightarrow \ell^+\ell^-$ decay, \mathcal{M} is sandwiched between vacuum and B_s meson states, from which the matrix elements $\langle 0 | \bar{s}\gamma_\mu(1-\gamma_5)b | B_s \rangle$ and $\langle 0 | \bar{s}\sigma_{\mu\nu}q^\nu(1+\gamma_5)b | B_s \rangle$ need to be calculated. These matrix elements are equal to

$$\begin{aligned} \langle 0 | \bar{s}\gamma^\mu(1-\gamma_5)b | B_s \rangle &= -if_{B_s}p_B^\mu , \\ \langle 0 | \bar{s}\sigma_{\mu\nu}q^\nu(1+\gamma_5)b | B_s \rangle &= 0 . \end{aligned} \quad (4)$$

Using these results, we get for the matrix element for $B_s \rightarrow \ell^+\ell^-$ decay

$$\mathcal{M} = i\frac{G\alpha}{\sqrt{2}\pi}V_{tb}V_{ts}^*m_\ell f_{B_s}C_{10}^{tot}(m_b)\bar{\ell}\gamma_5\ell . \quad (5)$$

Obviously, we see that the vector leptonic operator $\bar{\ell}\gamma_\mu\ell$ does not contribute to $B_s \rightarrow \ell^+\ell^-$ decay because it gives zero when contracted with B_s meson momentum.

Let us now turn our attention to the $B_s \rightarrow \ell^+\ell^-\gamma$ decay. The matrix element for the $b \rightarrow s\ell^+\ell^-\gamma$ decay can be obtained from that of the $b \rightarrow s\ell^+\ell^-$. For this purpose it is necessary to attach the photon to any charged internal as well as external line. When the photon is attached to internal lines, there will be a suppression factor of m_b^2/m_W^2 in the Wilson coefficient, since the resulting operators (dimension-8) are two order higher dimensionally than the usual ones (dimension-6). Thus the main contributions to the $b \rightarrow s\ell^+\ell^-\gamma$ decay come from diagrams when photon is radiated from initial (structure dependent SD part) and final (internal Bremsstrahlung IB part) fermions.

In order to calculate the matrix element corresponding to SD part, the following matrix elements must be calculated in the first hand

$$\begin{aligned} & \langle \gamma | \bar{s} \gamma_\mu (1 - \gamma_5) b | B_s \rangle , \\ & \langle \gamma | \bar{s} i \sigma_{\mu\nu} q^\nu (1 + \gamma_5) b | B_s \rangle . \end{aligned}$$

These matrix elements can be parametrized in terms of two independent, gauge invariant, parity conserving and parity violating form factors [11, 16] as

$$\langle \gamma | \bar{q} \gamma_\mu (1 - \gamma_5) b | B_s \rangle = \frac{e}{m_{B_s}^2} \left\{ \epsilon_{\mu\nu\lambda\sigma} \varepsilon^{*\nu} q^\lambda k^\sigma g(q^2) + i \left[\varepsilon_\mu^*(kq) - (\varepsilon^* q) k_\mu \right] f(q^2) \right\} , \quad (6)$$

$$\langle \gamma | \bar{s} i \sigma_{\mu\nu} q^\nu (1 + \gamma_5) b | B_s \rangle = \frac{e}{m_{B_s}^2} \left\{ \epsilon_{\mu\nu\lambda\sigma} \varepsilon^{*\nu} q^\lambda k^\sigma g_1(q^2) + i \left[\varepsilon_\mu^*(kq) - (\varepsilon^* q) k_\mu \right] f_1(q^2) \right\} , \quad (7)$$

where ε^μ and k^μ are the four-vector polarization and four-momentum of the photon, respectively, and q^μ is the momentum transfer. Using Eqs. (3), (6) and (7), matrix element describing the SD part takes the following form

$$\begin{aligned} \mathcal{M}_{SD} &= \frac{\alpha G_F}{2\sqrt{2}\pi} \frac{e}{m_{B_s}^2} V_{tb} V_{ts}^* \left\{ \epsilon_{\mu\nu\lambda\sigma} \varepsilon^{*\nu} q^\lambda k^\sigma \left[A_1 \bar{\ell} \gamma^\mu \ell + A_2 \bar{\ell} \gamma^\mu \gamma_5 \ell \right] \right. \\ &\quad \left. + i \left[\varepsilon_\mu^*(kq) - (\varepsilon^* q) k_\mu \right] \left[B_1 \bar{\ell} \gamma^\mu \ell + B_2 \bar{\ell} \gamma^\mu \gamma_5 \ell \right] \right\} , \end{aligned} \quad (8)$$

where

$$\begin{aligned} A_1 &= C_9^{tot} g(q^2) - 2C_7^{tot} \frac{m_b}{q^2} g_1(q^2) , \\ A_2 &= C_{10}^{tot} g(q^2) , \\ B_1 &= C_9^{tot} f(q^2) - 2C_7^{tot} \frac{m_b}{q^2} f_1(q^2) , \\ B_2 &= C_{10}^{tot} f(q^2) . \end{aligned}$$

When a photon is radiated from the final leptons, the corresponding matrix element is

$$\mathcal{M}_{IB} = \frac{\alpha G_F}{\sqrt{2}\pi} V_{tb} V_{ts}^* e f_{B_s} m_\ell C_{10}^{tot} \left[\bar{\ell} \left(\frac{\not{\varepsilon}^* \not{p}_{B_s}}{2p_1 k} - \frac{\not{p}_{B_s} \not{\varepsilon}^*}{2p_2 k} \right) \gamma_5 \ell \right] . \quad (9)$$

Finally the total matrix element for the $B_s \rightarrow \ell^+ \ell^- \gamma$ decay is equal to a sum of the Eqs. (8) and (9)

$$\mathcal{M} = \mathcal{M}_{SD} + \mathcal{M}_{IB} .$$

The double differential decay width of the $B_s \rightarrow \ell^+ \ell^- \gamma$ process, in the rest frame of the B_s meson, is

$$\frac{d\Gamma}{dE_\gamma dE_1} = \frac{1}{256\pi^3 m_{B_s}} |\overline{\mathcal{M}}|^2 , \quad (10)$$

where E_γ and E_1 are the energies of the photon and one of the final leptons, respectively, bar means that summation over spin of final particles is performed. The physical regions of E_γ and E_1 are determined from the following inequalities

$$0 \leq E_\gamma \leq \frac{m_{B_s}^2 - 4m_\ell^2}{2m_{B_s}},$$

$$\frac{m_{B_s} - E_\gamma}{2} - \frac{E_\gamma}{2}v \leq E_1 \leq \frac{m_{B_s} - E_\gamma}{2} + \frac{E_\gamma}{2}v, \quad (11)$$

where

$$v = \sqrt{1 - \frac{4m_\ell^2}{q^2}},$$

is the lepton velocity. The $|\mathcal{M}_{SD}|^2$ term is infrared divergence free, the interference term $2\text{Re}(\mathcal{M}_{SD}\mathcal{M}_{IB}^*)$ has integrable infrared singularity and only $|\mathcal{M}_{IB}|^2$ has infrared singularity due to the emission of soft photon. In the soft photon limit the $B_s \rightarrow \ell^+\ell^-\gamma$ decay cannot be distinguished from the pure leptonic $B_s \rightarrow \ell^+\ell^-$ decay. Therefore, in order to obtain a finite result the $B_s \rightarrow \ell^+\ell^-\gamma$ and the pure leptonic $B_s \rightarrow \ell^+\ell^-$ decay with radiative corrections must be considered together. It was shown in [17] that when both processes are considered together, all infrared singularities coming from the real photon emission and the virtual photon corrections are indeed canceled. However in the present work our point of view is slightly different, namely, instead of following the above mentioned procedure, we consider the $B_s \rightarrow \ell^+\ell^-\gamma$ decay as a separate process but not as the $\mathcal{O}(\alpha)$ correction to the $B_s \rightarrow \ell^+\ell^-$ decay. In other words, we consider the photon in the $B_s \rightarrow \ell^+\ell^-\gamma$ decay as a hard and detectable one. Therefore, in order to obtain the decay width we impose a cut on the photon energy, which will correspond to the experimental cut imposed on the minimum energy for the detectable photon. We require the photon energy to be larger than 25 MeV, i.e., $E_\gamma \geq \delta m_{B_s}/2$, where $\delta \geq 0.010$.

Using Eqs. (5) and (10) we get the following results for the $B_s \rightarrow \ell^+\ell^-$ and $B_s \rightarrow \ell^+\ell^-\gamma$ decays, respectively:

$$\mathcal{B}(B_s \rightarrow \ell^+\ell^-) = \frac{G_F^2 \alpha^2}{64\pi^2} m_{B_s}^3 \tau_{B_s} f_{B_s}^2 |V_{tb} V_{ts}^*|^2 \frac{4m_\ell^2}{m_{B_s}^2} \sqrt{1 - \frac{4m_\ell^2}{m_{B_s}^2}} |C_{10}^{tot}|^2 \quad (12)$$

$$\begin{aligned} \mathcal{B}(B_s \rightarrow \ell^+\ell^-\gamma) = & \left| \frac{G_F \alpha}{2\sqrt{2}\pi} \right|^2 |V_{tb} V_{ts}^*|^2 \frac{\alpha\pi}{(2\pi)^3} m_{B_s}^3 \tau_{B_s} \\ & \times \left\{ \int_0^{1-4r} dx x^3 v \left[(|A_1|^2 + |B_1|^2)(1-x+2r) + (|A_2|^2 + |B_2|^2)(1-x-4r) \right] \right. \\ & + 2r f_{B_s} C_{10}^{tot} \int_0^{1-4r} dx x^2 \text{Re}(A_1) \ln \frac{1+v}{1-v} \\ & \left. - 4 |f_{B_s} C_{10}^{tot}|^2 r \int_\delta^{1-4r} dx \left[2v \frac{1-x}{x} + \left(2 + \frac{4r}{x} - \frac{2}{x} - x \right) \ln \frac{1+v}{1-v} \right] \right\}, \quad (13) \end{aligned}$$

where $x = 2E_\gamma/m_{B_s}$ is the dimensionless photon energy and $r = m_\ell^2/m_{B_s}^2$.

It follows from Eq. (13) that to be able to calculate the decay width, the explicit forms of the form factors g , f , g_1 and f_1 are needed. In further analysis, use will be made of the form factors that are predicted by the light-cone QCD sum rules [11, 16], whose q^2 dependences, to a very good accuracy, can be written in the following dipole forms,

$$\begin{aligned} g(q^2) &= \frac{1 \text{ GeV}}{\left(1 - \frac{q^2}{(5.6 \text{ GeV})^2}\right)^2}, & f(q^2) &= \frac{0.8 \text{ GeV}}{\left(1 - \frac{q^2}{(6.5 \text{ GeV})^2}\right)^2}, \\ g_1(q^2) &= \frac{3.74 \text{ GeV}^2}{\left(1 - \frac{q^2}{40.5 \text{ GeV}^2}\right)^2}, & f_1(q^2) &= \frac{0.68 \text{ GeV}^2}{\left(1 - \frac{q^2}{30 \text{ GeV}^2}\right)^2}. \end{aligned} \quad (14)$$

As is obvious from Eq. (2), to get numerical values of the branching ratios the value of the fourth generation CKM matrix element $|V_{tb}V_{ts}^*|$ is needed. For this purpose we will use the experimentally measured values of the branching ratios $\mathcal{B}(B \rightarrow X_s \gamma)$ and $\mathcal{B}(B \rightarrow X_c e \bar{\nu}_e)$. In order to reduce the uncertainties coming from b quark mass, we consider the ratio

$$R = \frac{\mathcal{B}(B \rightarrow X_s \gamma)}{\mathcal{B}(B \rightarrow X_c e \bar{\nu}_e)}. \quad (15)$$

In leading logarithmic approximation this ratio can be written as

$$R = \frac{6\alpha |C_7^{tot}(m_b)V_{tb}V_{ts}^*|^2}{\pi f(\hat{m}_c)\kappa(\hat{m}_c)|V_{cb}|^2}, \quad (16)$$

where $\hat{m}_c = m_c/m_b$ and the phase factor $f(\hat{m}_c)$ and $\mathcal{O}(\alpha_s)$ QCD correction factor $\kappa(\hat{m}_c)$ [18] of $b \rightarrow c \ell \bar{\nu}$ are given by

$$\begin{aligned} f(\hat{m}_c) &= 1 - 8\hat{m}_c^2 + 8\hat{m}_c^6 - \hat{m}_c^8 - 24\hat{m}_c^4 \ln(\hat{m}_c), \\ \kappa(\hat{m}_c) &= 1 - \frac{2\alpha_s(m_b)}{3\pi} \left[\left(\pi^2 - \frac{31}{4} \right) (1 - \hat{m}_c^2)^2 + \frac{3}{2} \right]. \end{aligned} \quad (17)$$

From Eqs. (16) and (15) we get

$$\left| C_7^{SM} V_{tb} V_{ts}^* + C_7^{new} V_{t'b} V_{t's}^* \right| = \sqrt{\frac{\pi f(\hat{m}_c) \kappa(\hat{m}_c) |V_{cb}|^2}{6\alpha} \frac{\mathcal{B}(B \rightarrow X_s \gamma)}{\mathcal{B}(B \rightarrow X_c e \bar{\nu}_e)}}. \quad (18)$$

The model parameters can be constrained from the measured branching ratio of the $B \rightarrow X_s \gamma$ decay

$$\mathcal{B}(B \rightarrow X_s \gamma) = \begin{cases} (3.21 \pm 0.43 \pm 0.27_{-0.10}^{+0.18}) \times 10^{-4} & [19] \\ (3.36 \pm 0.53 \pm 0.42 \pm 0.54) \times 10^{-4} & [20] \\ (3.11 \pm 0.80 \pm 0.72) \times 10^{-4} & [21] \end{cases}$$

In further numerical analysis, we will use the weighted average value $\mathcal{B}(B \rightarrow X_s \gamma) = (3.23 \pm 0.42) \times 10^{-4}$ [22] for the branching ratio of the $B \rightarrow X_s \gamma$ decay.

Next constraint to the extended CKM matrix element comes from the unitarity condition, i.e.,

$$\begin{aligned} |V_{us}|^2 + |V_{cs}|^2 + |V_{ts}|^2 + |V_{t's}|^2 &= 1, \\ |V_{ub}|^2 + |V_{cb}|^2 + |V_{tb}|^2 + |V_{t'b}|^2 &= 1, \\ V_{ub}V_{us}^* + V_{cb}V_{cs}^* + V_{tb}V_{ts}^* + V_{t'b}V_{t's}^* &= 0. \end{aligned} \quad (19)$$

At this point we would like to make the following remark: Charged-current three-level decays are well measured experimentally and they are not affected by new physics at leading order. For this reason, in the following discussions we will use Particle Data Group (PDG) constraints [10] for $|V_{ud}|$, $|V_{us}|$, $|V_{cs}|$, $|V_{cb}|$ and $|V_{ub}/V_{cb}|$. Using the weighted average for $\mathcal{B}(B \rightarrow X_s \gamma)$ and PDG constraint $0.38 \leq |V_{cb}| \leq 0.044$ [10], from Eqs. (18) and (19) we obtain the following constraints

$$0.011 \leq |C_7^{SM} V_{tb} V_{ts}^* + C_7^{new} V_{t'b} V_{t's}^*| \leq 0.015, \quad (20)$$

$$0.03753 \leq |V_{tb} V_{ts}^* + V_{t'b} V_{t's}^*| \leq 0.043976, \quad (21)$$

$$0 \leq |V_{ts}|^2 + |V_{t's}|^2 \leq 0.00492, \quad (22)$$

$$0.998 \leq |V_{tb}|^2 + |V_{t'b}|^2 \leq 0.9985. \quad (23)$$

3 Numerical analysis

In this section we study the constraint on $V_{t'b} V_{t's}^*$ and using the resulting bound on $|V_{t'b} V_{t's}^*|$ we investigate the influence of fourth generation on the branching ratios. Before performing this analysis we present the values of the main input parameters which we use in our calculations: $m_b = 4.8 \text{ GeV}$, $m_c = 1.35 \text{ GeV}$, $m_{B_s} = 5.369 \text{ GeV}$, $\tau_{B_s} = 1.64 \times 10^{-12} \text{ s}$. Furthermore in calculating the branching ratios the values of the Wilson coefficients $C_7^{SM}(m_b)$, $C_9^{SM}(m_b)$ and $C_{10}^{SM}(m_b)$ are needed. In leading logarithmic approximation $C_7^{SM}(m_b) = -0.315$ and $C_{10}^{SM}(m_b) = -4.642$ (see [14, 15]). The analytic expression of $C_9^{SM}(m_b)$ is given as

$$\begin{aligned} C_9^{SM}(m_b) &= 4.227 + g(\hat{m}_c, \hat{s})(3C_1 + C_2 + 3C_3 + C_4 + 3C_5 + C_6) \\ &- \frac{1}{2}g(0, \hat{s})(C_3 + 3C_4) - \frac{1}{2}g(1, \hat{s})(4C_3 + 4C_4 + 3C_5 + C_6) \\ &+ \frac{2}{9}(3C_3 + C_4 + 3C_5 + C_6), \end{aligned}$$

where $\hat{s} = q^2/m_b^2$. The explicit form of the expressions for the functions $g(\hat{m}_i, \hat{s})$ and the values of the individual Wilson coefficients can be found in [14, 15].

It should be noted that $B_s \rightarrow \ell^+ \ell^- \gamma$ can also receive long distance contributions which have their origin in the real intermediate states, i.e., J/ψ , ψ' , \dots . In the present work we neglect such long distance contributions.

In order to study the influence of the fourth generation quarks to the rare $B_s \rightarrow \ell^+ \ell^-$ and $B_s \rightarrow \ell^+ \ell^- \gamma$ decays we need the values of $V_{tb} V_{ts}^*$ and $V_{t'b} V_{t's}^*$. For this purpose we carry out the following analysis. We consider $V_{tb} V_{ts}^*$ and $V_{t'b} V_{t's}^*$ to be two independent

complex parameters. They are constrained by the unitarity condition (19) and the measured experimental value on branching ratio of the $B \rightarrow X_s \gamma$ decay (see Eq. (20)) which depends on $m_{t'}$. Thus for each value of $m_{t'}$ there exists an allowed region in the $(|V_{tb}V_{ts}^*| \text{ and } |V_{t'b}V_{t's}^*|)$ plane.

It is not possible to solve the constraints Eqs. (20)-(23) analytically. Therefore, we chose a large number of random *complex* values for V_{tb} , V_{ts} , $V_{t'b}$, $V_{t's}$ such that the constraints are all satisfied. For a sufficiently large number, the selected values would range over the whole solution space. In Figs. (1)–(3), to give an idea about the solution space, we present the allowed region in the plane of the absolute values of $V_{tb}V_{ts}^*$ and $V_{t'b}V_{t's}^*$ at $m_{t'} = 200 \text{ GeV}$, $m_{t'} = 300 \text{ GeV}$, and $m_{t'} = 300 \text{ GeV}$, respectively. The upper left boundary of the allowed region is determined by Eq. (22) and (23) whereas the other three boundaries are determined by Eqs. (20) and (21). From these figures it can easily be seen that, when $|V_{t'b}V_{t's}^*| \simeq 0$ the value of $|V_{tb}V_{ts}^*|$ is close to its SM value and is evenly distributed around 0.04. However, when the value of $|V_{t'b}V_{t's}^*|$ gets larger, up to a critical value around $|V_{t'b}V_{t's}^*| \sim 0.012$, the allowed region for $|V_{tb}V_{ts}^*|$ becomes wider with the center fixed at 0.04. Beyond the critical point, the center of the region shifts toward smaller values with its width fixed. This behavior of the allowed range for $|V_{tb}V_{ts}^*|$ continues until $|V_{t'b}V_{t's}^*|$ reaches a second critical value around $|V_{t'b}V_{t's}^*| \sim 0.04$. When $|V_{t'b}V_{t's}^*|$ takes values beyond this value, the allowed region for $|V_{tb}V_{ts}^*|$ begins to shrink to zero with its center fixed around 0.012. Similar behavior is observed for all other values of $m_{t'}$. After determining the physical regions for $V_{tb}V_{ts}^*$ and $V_{t'b}V_{t's}^*$, the range of the region for the branching ratio of the $B_s \rightarrow \ell^+\ell^-$ and $B_s \rightarrow \ell^+\ell^-\gamma$ decays can be determined. Depicted in Figs. (4) and (5) are the dependence of the ranges of the branching ratios of the $B_s \rightarrow \mu^+\mu^-$ and $B_s \rightarrow \tau^+\tau^-$ decays on $m_{t'}$, respectively. It is evident from both figures that at lower values of $m_{t'}$ ($200 \text{ GeV} \leq m_{t'} \leq 250 \text{ GeV}$) the branching value is distributed mainly around the SM value. This is to be expected since when $m_{t'} = m_t$, the contributions to the Wilson coefficients from the new physics effects are identical to those from the SM. In particular, after dividing Eq. (20) by $|C_7^{SM}|$, Eq. (20) becomes a constraint on $|V_{tb}V_{ts}^* + V_{t'b}V_{t's}^*|$ just as Eq. (21), and the branching ratio itself also depends on this combination only. Obviously, for larger values of $m_{t'}$ the possible departure from the SM prediction becomes substantial, signaling the existence of new physics beyond SM.

It follows from these figures that there exists a region for $V_{tb}V_{ts}^*$ and $V_{t'b}V_{t's}^*$ where branching ratio attains smaller values than the SM prediction for all values of $m_{t'}$. This can be explained as follows. It follows from Eq. (12) that the branching ratio is proportional to

$$\mathcal{B}(B_s \rightarrow \ell^+\ell^-) \propto |C_{10}^{tot}|^2 |V_{tb}V_{ts}^*|^2 \equiv |C_{10}^{SM}|^2 \left| 1 + \frac{V_{t'b}V_{t's}^*}{V_{tb}V_{ts}^*} \frac{C_{10}^{new}}{C_{10}^{SM}} \right|^2 |V_{tb}V_{ts}^*|^2 .$$

The ratio C_{10}^{new}/C_{10}^{SM} is positive for all values of $m_{t'}$ and increases with increasing $m_{t'}$. From Eq. (24), we see that depending on whether $|1 + \lambda|$, where

$$\lambda = \frac{V_{t'b}V_{t's}^*}{V_{tb}V_{ts}^*} \frac{C_{10}^{new}}{C_{10}^{SM}} ,$$

is greater than, equal to, or less than one, the branching ratio is greater than, equal to, or less than the SM value. The boundary separating these regions, $|1 + \lambda| = 1$ can be

considered as a circle on the complex λ plane with radius 1 and center at -1 . Within this circle, the predicted branching ratio is smaller than the SM value, whereas out of this circle, it is bigger.

The dependence of the branching ratio on $m_{t'}$ for the $B_s \rightarrow \mu^+\mu^-\gamma$ and $B_s \rightarrow \tau^+\tau^-\gamma$ decays are shown in Figs. (6) and (7). Qualitative understanding of the dependence of the branching ratio on $m_{t'}$ for the $B_s \rightarrow \ell^+\ell^-\gamma$ ($\ell = \mu, \tau$) is analogous to the $B_s \rightarrow \ell^+\ell^-$ ($\ell = \mu, \tau$) case. The lower bound of x is chosen to be $x = 0.01$ in order to get finite result for the $\mathcal{B}(B_s \rightarrow \ell^+\ell^-\gamma)$ decay (see Eq. (13)). It should be noted here that the branching ratio for the $B_s \rightarrow \mu^+\mu^-\gamma$ decay practically is insensitive to the variation of x_{min} . For example when x_{min} is varied from 10^{-3} to 10^{-1} , the branching ratio changes only about $\sim 5\%$.

Our final remark is that fourth generation can give contribution to the rare B and K decays. For this reason constraints on fourth generation imposed by the ρ parameter, Δm_K , ε_K , $B_{d(s)}^0 - \bar{B}_{d(s)}^0$ mixing, $K_L \rightarrow \pi^0\nu\bar{\nu}$, $K_L \rightarrow \mu^+\mu^-$ decays, must be considered together with $b \rightarrow s\gamma$ decay. Early attempts in this direction were done in [22]. A more detailed analysis of constraints arising from rare B and K meson decays is presently under study.

In conclusion, we have studied the effect of the fourth generation quarks to the rare $B_s \rightarrow \ell^+\ell^-$ and $B_s \rightarrow \ell^+\ell^-\gamma$ decays. From the experimental result for the branching ratio of $B \rightarrow X_s\gamma$ decay, the values of $|V_{tb}V_{ts}^*|$ and $|V_{t'b}V_{t's}^*|$ are constrained. We have observed that, depending on the relative phase between $V_{tb}V_{ts}^*$ and $V_{t'b}V_{t's}^*$, fourth generation quarks can enhance or suppress the SM result. As a result the branching ratios of $B_s \rightarrow \ell^+\ell^-$ and $B_s \rightarrow \ell^+\ell^-\gamma$ decays can be larger or smaller compared to that of the SM prediction.

References

- [1] D. Boutigny *et al.*, BaBar Technical design report, SLAC-R-0457;
M. T. Cheng *et al.*, BELLE Collaboration, a study of CP violation in B meson decays: Technical design report, BELLE-TDR-3-95;
K. T. Pitts *et al.*, D0 Collaboration and CDF Collaboration, FERMILAB-CONF-98-380-E, Oct 1998. 17pp. To be published in the proceedings of 4th Workshop on Heavy Quarks at Fixed Target (HQ 98), Batavia, IL, 10–12 Oct 1998;
P. Krizan *et al.*, HERA-B Collaboration, *Nucl. Inst. Meth.* **A351** (1994) 111;
D. Websdale *et al.*, LHC-B Collaboration, *Nucl. Phys. Proc. Suppl.* **50** (1996) 333.
- [2] W. Skiba and J. Kalinowski, *Nucl. Phys.* **B304** (1993) 3.
- [3] D. Atwood, L. Reina, A. Soni, *Phys. Rev.* **D55** (1997) 3156.
- [4] H. E. Logan and U. Nierste, *Nucl. Phys.* **B586** (2000) 39.
- [5] K. S. Babu and C. Kolda, *Phys. Rev. Lett.* **84** (2000) 228.
- [6] C-S. Huang, W. Liao, Q-S. Yan, S-H. Zhu *Phys. Rev.* **D63** (2001) 114021.
- [7] P. H. Chankowski, L. Slawianowska, *Phys. Rev.* **D63** (2001) 054012.
- [8] E. O. Iltan, G. Turan, prep: **hep-ph/0011005** (2000).
- [9] X. G. He, T. D. Nguyen, R. R. Volkas, *Phys. Rev.* **D38** (1988) 814.
- [10] K. Hagiwara *et al.*, Particle Data Group, *Phys. Rev.* **D66** (2002) 010001.
- [11] T. M. Aliev, A. Özpıneci and M. Savcı, *Phys. Rev.* **D55** (1997) 7059.
- [12] G. Eilam, C. D. Lü, D. X. Zhang, *Phys. Lett.* **B391** (1997) 461.
- [13] M. Maltoni *et al.*, *Phys. Lett.* **B476** (2000) 176.
- [14] G. Buchalla and A. J. Buras, *Nucl. Phys.* **B400** (1993) 225.
- [15] M. Misiak, *Nucl. Phys.* **B398** (1993) 23; Erratum: *ibid.* **B439** (1995) 461.
- [16] G. Eilam, I. Halperin and R. R. Mendel *Phys. Lett.* **B361** (1995) 137.
- [17] T. M. Aliev, N. K. Pak and M. Savcı, *Phys. Lett.* **B424** (1998) 175.
- [18] A. J. Buras, prep: hep-ph/9806471 (1998).
- [19] S. Chen *et al.*, CLEO Collaboration, *Phys. Rev. Lett.* **87** (2001) 251807.
- [20] H. Tajima, BELLE Collaboration, prep: **hep-ex/0111037** (2001).
- [21] R. Barate *et al.*, ALEPH Collaboration, *Phys. Lett.* **B429** (1998) 169.
- [22] P. Cambino, M. Misiak, *Nucl. Phys.* **B611** (2001) 338.
- [23] T. Hattori, T. Hasuiko, S. Wakaizumi, prep: **hep-ph/9804412** (1998).

Figure captions

Fig. (1) The allowed regions for $|V_{tb}V_{ts}^*|$ and $|V_{t'b}V_{t's}^*|$ at $m_{t'} = 200 \text{ GeV}$.

Fig. (2) The same as in Fig. (1), but at $m_{t'} = 300 \text{ GeV}$.

Fig. (3) The same as in Fig. (1), but at $m_{t'} = 400 \text{ GeV}$.

Fig. (4) The dependence of the branching ratio for the $B_s \rightarrow \mu^+\mu^-$ decay on the fourth up quark mass $m_{t'}$.

Fig. (5) The same as in Fig. (4), but for the $B_s \rightarrow \tau^+\tau^-$ decay.

Fig. (6) The same as in Fig. (4), but for the $B_s \rightarrow \mu^+\mu^-\gamma$ decay.

Fig. (7) The same as in Fig. (4), but for the $B_s \rightarrow \tau^+\tau^-\gamma$ decay.

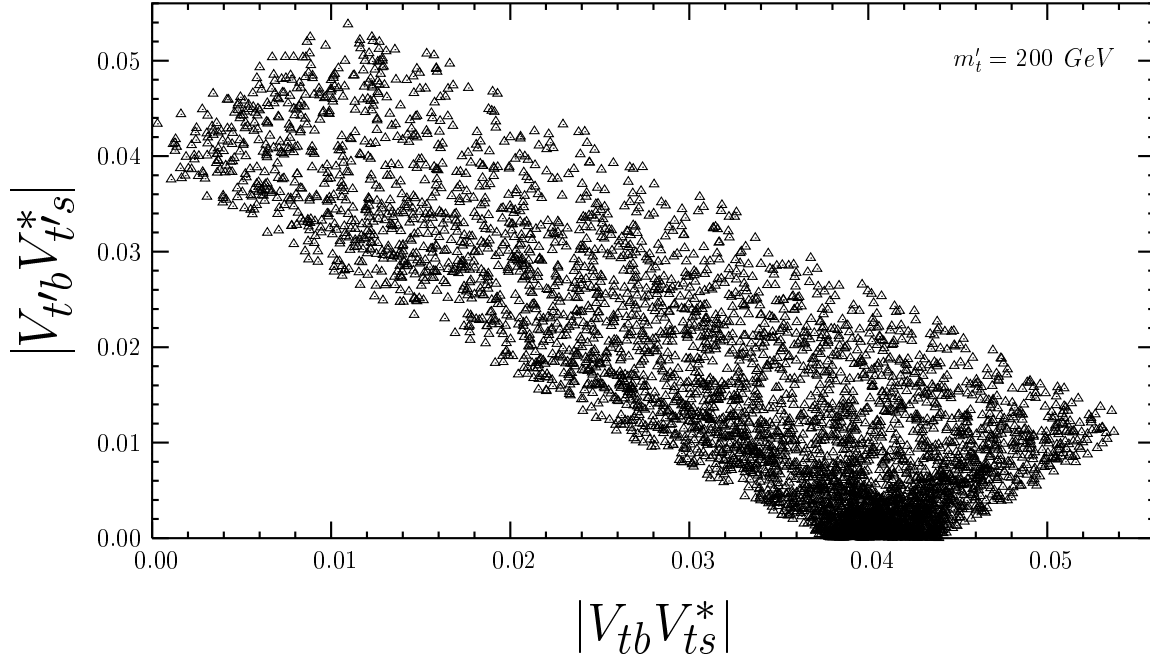


Figure 1:

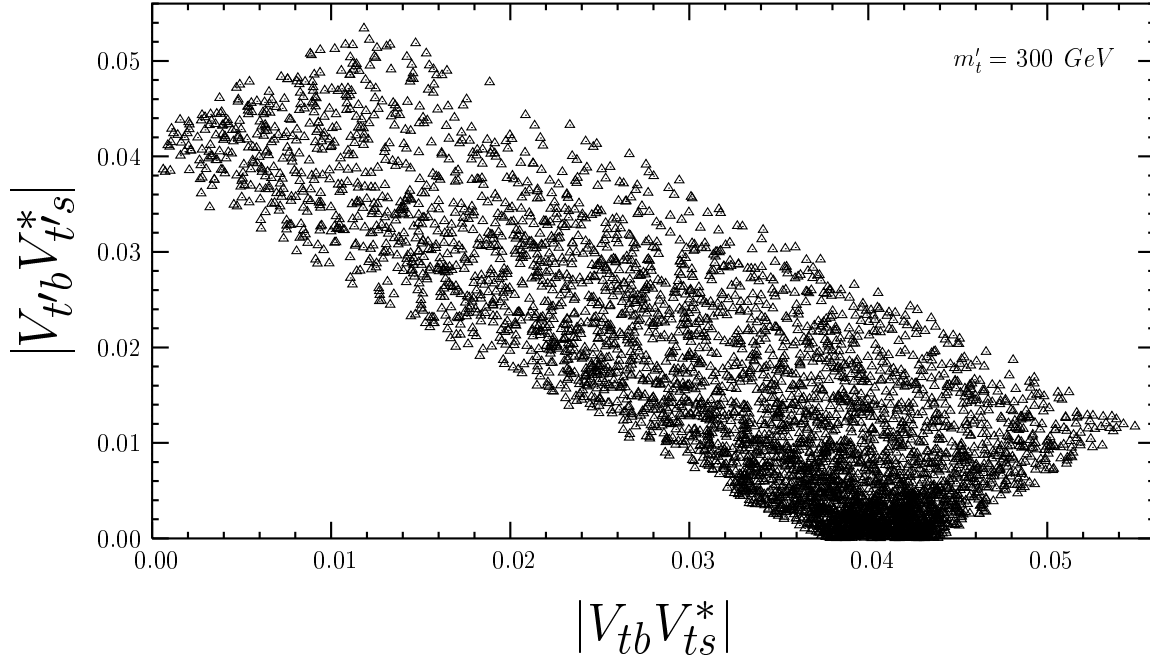


Figure 2:

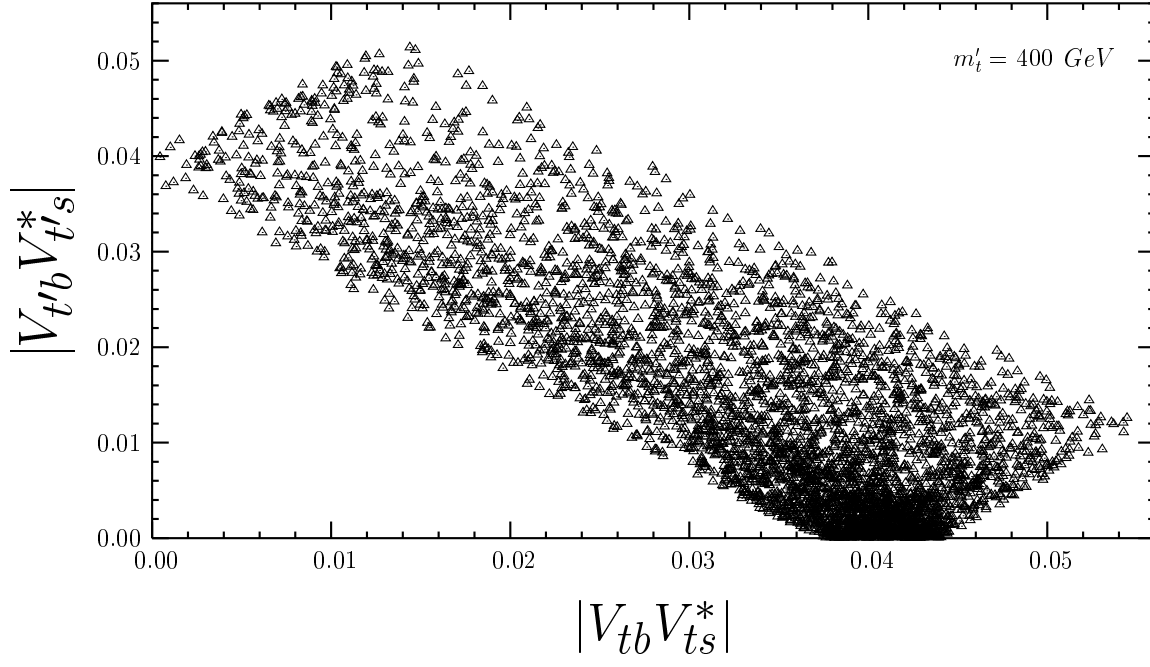


Figure 3:

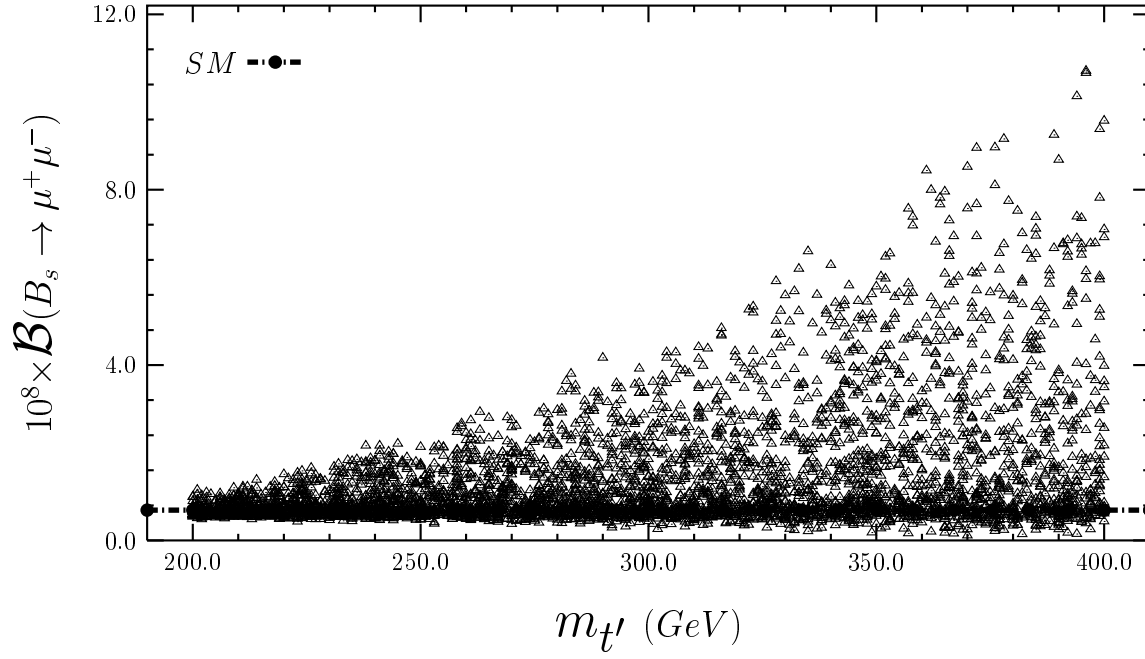


Figure 4:

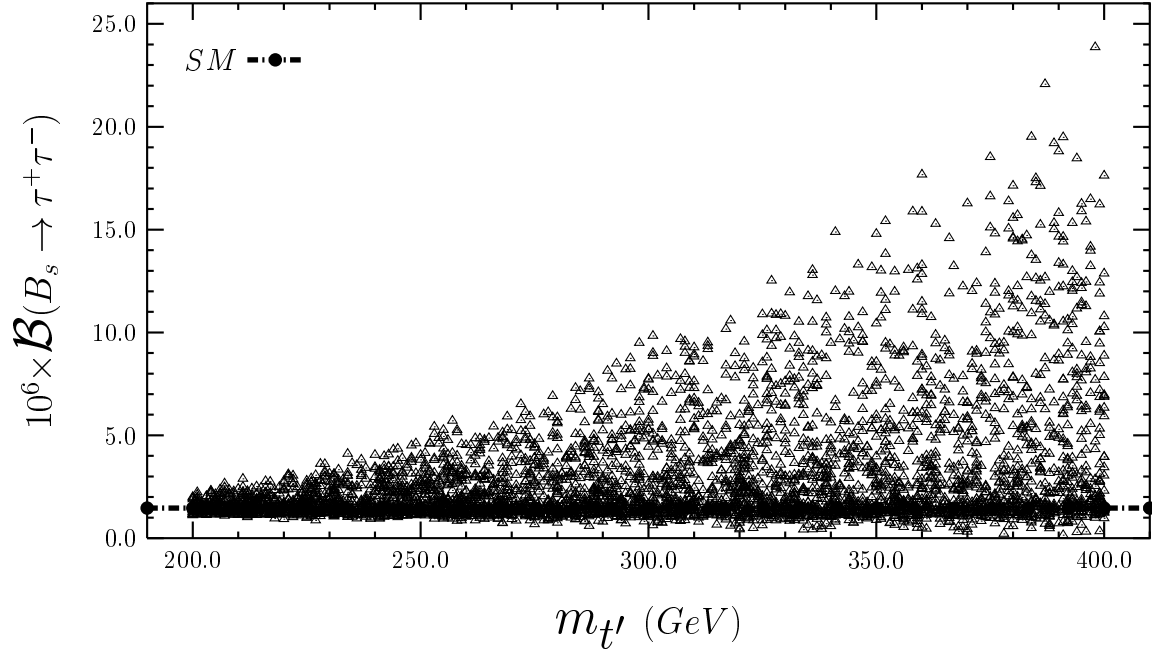


Figure 5:

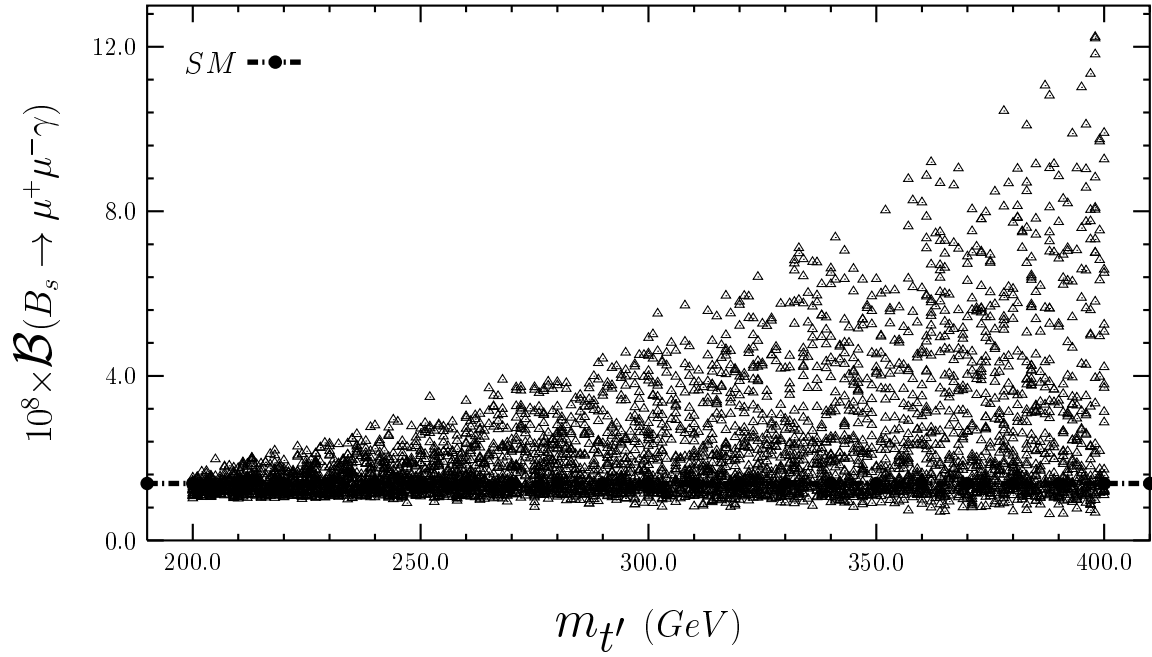


Figure 6:

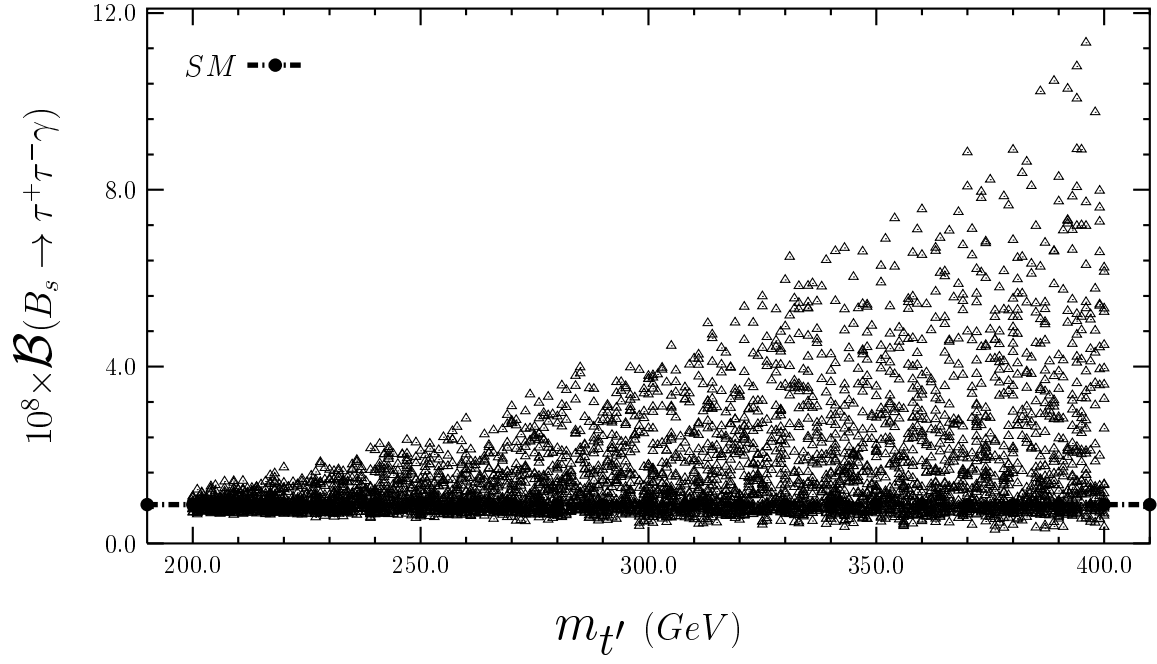


Figure 7: